Potassium Conductance of the Squid Giant Axon

Single-Channel Studies

ISABEL LLANO, CHRISTINA K. WEBB, AND FRANCISCO BEZANILLA

From the Department of Physiology, Ahmanson Laboratory of Neurobiology and Jerry Lewis Neuromuscular Research Center, University of California, Los Angeles, California 90024; the Marine Biological Laboratory, Woods Hole, Massachusetts 02543; and the Catalina Marine Science Center, Avalon, California 90704

ABSTRACT The patch-clamp technique was implemented in the cut-open squid giant axon and used to record single K channels. We present evidence for the existence of three distinct types of channel activities. In patches that contained three to eight channels, ensemble fluctuation analysis was performed to obtain an estimate of 17.4 pS for the single-channel conductance. Averaged currents obtained from these multichannel patches had a time course of activation similar to that of macroscopic K currents recorded from perfused squid giant axons. In patches where single events could be recorded, it was possible to find channels with conductances of 10, 20, and 40 pS. The channel most frequently encountered was the 20-pS channel; for a pulse to 50 mV, this channel had a probability of being open of 0.9. In other single-channel patches, a channel with a conductance of 40 pS was present. The activity of this channel varied from patch to patch. In some patches, it showed a very low probability of being open (0.16 for a pulse to 50 mV) and had a pronounced lag in its activation time course. In other patches, the 40-pS channel had a much higher probability of being open (0.75 at a holding potential of 50 mV). The 40-pS channel was found to be quite selective for K over Na. In some experiments, the cut-open axon was exposed to a solution containing no K for several minutes. A channel with a conductance of 10 pS was more frequently observed after this treatment. Our study shows that the macroscopic K conductance is a composite of several K channel types, but the relative contribution of each type is not yet clear. The time course of activation of the 20-pS channel and the ability to render it refractory to activation only by holding the membrane potential at a positive potential for several seconds makes it likely that it is the predominant channel contributing to the delayed rectifier conductance.

INTRODUCTION

Since the classic work of Hodgkin and Huxley (1952) describing the membrane conductances that underlie the generation and propagation of the nerve impulse, the

Address reprint requests to Dr. Isabel Llano, Laboratoire de Neurobiologie, Ecole Normale Superieure, 46 rue d'Ulm, 75230, Paris Cedex 05, France.

J. GEN. PHYSIOL. © The Rockefeller University Press · 0022-1295/88/08/0179/18 $2.00
Volume 92 August 1988 179–196

squid giant axon preparation has yielded a great deal of information on the properties of the ionic channels responsible for these conductance changes. This information has been derived from the study of both macroscopic ionic currents and gating currents, which can be recorded with a high degree of resolution in this preparation (Armstrong, 1981; Bezanilla, 1985*a*). It is clear that studies of the properties of these conductances at the single-channel level will aid in understanding how these entities function at the molecular level. Although the first recordings of unitary currents flowing through voltage-gated channels were performed in squid axons (Conti and Neher, 1980), the difficulty in forming high-resistance seals in this preparation has precluded, until recently, more detailed studies of this type.

In this article, we report the implementation of patch-clamp techniques for the recording of K single-channel currents from the inside surface of cut-open squid giant axons. Our results reveal three distinct types of K channel activity in this preparation, the properties of which are described. Some of these results have been presented in abstract form (Llano and Bezanilla, 1985).

METHODS

The giant axon of the squids *Loligo pealei* and *L. opalescens* was used for these experiments. The procedure for obtaining pieces of axonal membrane was based on a modification of the cut-open axon preparation (Llano and Bezanilla, 1980) that had originally been implemented for the recording of current fluctuations (Levis et al., 1984). A brief description of the technique has been presented with results on single Na channels (Bezanilla, 1987).

Patch Clamp of the Cut-Open Axon

A piece of axon up to 1 cm long, cleaned of connective tissue, was tied at both ends and pinned to a thin layer of Sylgard covering the bottom of the experimental chamber. During the first series of experiments, the chamber was a 3.5-cm plastic petri dish; in more recent experiments, the petri dish was replaced by a rectangular chamber made of thin Lucite with a coverslip as the bottom. While bathed in artificial seawater (ASW; composition: 440 mM NaCl, 10 mM $CaCl_2$, by endogenous Ca-sensitive proteases; 50 mM $MgCl_2$, 10 mM HEPES, 0–10 mM KCl, as indicated in the figure legends), the axon was cut longitudinally with microscissors to expose the internal surface of the membrane. The resulting axonal sheet was then perfused for 3–5 min with ASW at room temperature to wash out as much of the axoplasm as possible (e.g., Hodgkin and Katz, 1949) (Pant and Gainer, 1980). After this procedure, ASW was maintained in the recording chamber. In some cases, the ASW was replaced with a solution containing one-fourth of the normal $CaCl_2$ and $MgCl_2$ (low-divalent ASW); the axon was maintained in this solution for the remainder of the experiment. Both the external and internal surfaces of the axonal membrane were continuously exposed to either normal or low-divalent ASW until seal formation. All external solutions contained 200 nM tetrodotoxin (Sigma Chemical Co., St. Louis, MO) in order to block Na channels. The pH of the external and internal solutions was adjusted to 7.6 and 7.3, respectively, and the osmolarity was adjusted to 1,000 and 980 mosmol, respectively.

The experimental set-up (see Fig. 1) consisted of an inverted compound microscope mounted on an *X-Y* table that permitted the microscope to be moved with respect to the preparation and allowed for easy scanning of membrane areas, which appeared to be clean of axoplasm and other debris. The normal microscope stage was removed and replaced by a fixed metal stand, which held both the chamber and the micromanipulator carrying the patch

pipette. The temperature of the chamber containing the axonal sheet was maintained constant by an aluminum block in thermal contact with four small Peltier units. The Peltier units dissipated the heat directly to the aluminum plate that replaced the microscope stage and they were fed by a custom-made temperature controller, which measured the temperature of the aluminum block in contact with the chamber. The temperature of the bath was maintained between 13 and 25°C. The micromanipulator was assembled from micropositioning stages driven by manual and motorized drives (Newport Corp., Fountain Valley, CA). The set-up was mounted on a pneumatic isolation system.

All the experiments reported here were done using the excised outside-out configuration of the patch-clamp technique (Hamill et al., 1981). In the cut-open axon preparation, this configuration was achieved by moving a patch pipette close to the internal surface of the

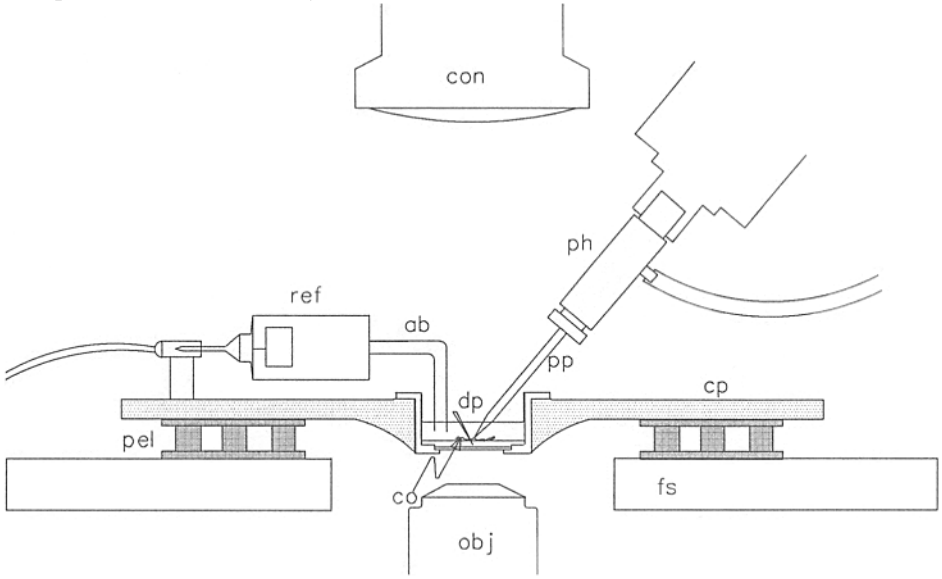

FIGURE 1. Schematic drawing of the experimental set-up to show details of the cooler, chamber, and miscroscope objective and condenser. The condenser can be tilted back to allow the positioning of a dissecting microscope used to cut the axon open. Abbreviations: ab, agar bridge; co, cut-open axon; con, microscope condenser; cp, cooling plate; dp, steel pin to hold the axon on the Sylgard; fs, fixed stage; pel; Peltier cooler; ph, pipette holder; pp, patch pipette; rf, reference electrode. For explanations, see text.

membrane, applying slight suction to secure seal formation, and then withdrawing the pipette from the axonal sheet. Similar results were also obtained in the cell-attached configuration, in which the pipette remained attached to the axonal sheet. The pipette used for patch recording was filled with a solution containing 490 mM K-glutamate, 25 mM K-fluoride, 5 mM KCl, 10 mM K-HEPES, and 10 mM K-EGTA. The total internal concentration of K^+ was lower in some experiments; in these cases, sucrose was added to maintain constant osmotic pressure. For experiments in which the selectivity of the channels was studied, the external solution contained 400 mM KCl, 130 mM NaCl, 12.5 mM $MgCl_2$, 2.5 mM $CaCl_2$, and 10 mM Tris. In our figure legends, solutions are identified as *x*K-ASW//*y*K, where *x* and *y* define the total concentration of K^+ in the external and internal solutions, respectively.

The conditions described above seemed to aid seal formation significantly in this preparation. High-resistance seals (>10 GΩ) were stable for up to several hours. However, patches were often completely silent, and on several occasions the single-channel activity observed immediately after excision of a patch disappeared within a few minutes. The results presented in this article were gathered from patches in which both the seal resistance and channel activity were stable for at least 30 min.

Patch currents were recorded with a current-to-voltage converter that followed the design of Sigworth (1983), with a feedback resistor of either 50 or 100 GΩ. Some experiments were done using a head-stage built with discrete parts; in this case, the holding potential and pulses were applied to the bath while the interior of the pipette was maintained at virtual ground. In other experiments, we used an Axopatch (Axon Instruments, Inc., Burlington, CA). In all cases, a two-stage frequency booster was used to extend the frequency response of the converter to a final bandwidth of 7.5 kHz. Analog compensation of capacitive transients was applied to all current records. These were subsequently filtered with a six-pole Bessel filter at a corner frequency of 5 kHz, digitized, and stored on disk for analysis.

Pulse Generation, Data Acquisition, and Analysis

The system for pulse generation, data acquisition, and storage was based on an IBM AT microcomputer with a custom-made interface for acquisition and waveform generation, which followed the design of the system used by Stimers et al. (1987). Waveforms were generated by the computer and stored in a double-ported memory that could be accessed by the central processing unit (CPU) of the computer or by the optoisolated D/A converter that generated the actual analog waveforms to be applied to the patch clamp. The acquisition was done via a 16-bit A/D converter connected through optoisolators to another double-ported memory, which would be accessed by either the optoisolated A/D converter or the computer CPU. This system of acquisition was used routinely for pulsed data, and the collected digitized currents were stored in magnetic media. For continuous acquisition, the data were stored in a modified digital audio processor connected to a VCR (see Bezanilla, 1985*b*).

Analysis of continuous recordings was not done directly from the VCR tape; rather, portions of the tape were transferred to the computer using the acquisition system described above. The double-ported memory in the computer interface board was divided into two parts. While one portion of the memory was being filled by the data on the tape, the other was being dumped into a high-capacity cartridge disk (Bernouilli Box, Ogden, UT), thus allowing a continuous transfer of data into a magnetic medium having random access capabilities.

The analysis of single-channel fluctuations was performed on the same computer as that used for data acqusition, waveform generation, and data storage. The analysis programs were written in a combination of FORTRAN and assembly languages. Pulsed data were first scanned to locate blank records, and then these were averaged and subtracted from the rest of the traces. Point-by-point amplitude histograms of each trace were made and the peaks and valleys of the histograms were used to set the threshold for automatic detection of transitions. The level for threshold detection was set at 50% of the mean single-channel current level determined from the amplitude histograms. For each trace analyzed, an idealized trace was automatically created based on the open and closed current levels and the transition threshold determined from the amplitude histogram. Events that were terminated by the end of the voltage pulse were discarded. If this simulation was accepted as a good representation of the original data, then the idealized trace was stored. Open, closed, and first latency times were then obtained from the idealized traces. Amplitude and open- or closed-time histograms were fitted by least-squares minimization using a simplex algorithm. Amplitude histograms

were fitted to a sum of Gaussian functions of the form

$$n = \sum_k a_k \exp\{-[(i - x_k)/b_k]^2\},$$

where i is current amplitude, n is number of events at that particular amplitude, and a_k, x_k, and b_k are parameters describing the amplitude, mean, and dispersion of the Gaussian function.

Continuous recordings were analyzed in a similar way, except that blank records were not averaged and subtracted. Rarely, periods during which all channel activity stopped for lengths of time exceeding 5 s were observed for the large-conductance channel at potentials >10 mV. These "silent periods" were not included in the determination of open probability.

In general, single-channel conductance is expressed as chord conductance, $G = i/(V - V_K)$, where V_K is the K reversal potential. A ratio of 0.025 was assumed for the permeabilities P_{Na}/P_K (Latorre and Miller, 1983). The chord conductance has been used in view of the evidence that the single-channel current-voltage relation for some types of K channels is not linear under physiological K gradients (e.g., Standen et al., 1985).

RESULTS

Multichannel Patches

Excised patches obtained from cut-open axons maintained in ASW with K^+ concentrations of 5–10 mM displayed outward current fluctuations upon depolarization, the properties of which were consistent with the activation of the delayed rectifier K channels. Under these ionic conditions, most patches had at least three or four active channels. In these multichannel patches, ensemble fluctuation analysis (Sigworth, 1980) was performed in order to estimate the value of the single-channel conductance. Fig. 2 *A* shows the mean current (upper trace) and the associated ensemble variance (lower trace) calculated from a set of 200 depolarizations from −80 to 80 mV. The plot of variance (S^2) as a function of mean current (I), shown in Fig. 2 *B*, was fitted well by a parabolic curve according to the equation $S^2(t) = iI(t) - I(t)^2/N$, yielding a value of 2.7 pA for the single-channel current (i) and 8 for the number of channels (N). The estimated value of the single-channel conductance was 17.4 pS.

The channels giving rise to the current in multichannel patches activate in a voltage-dependent manner, as evidenced by inspection of the averaged currents obtained at different membrane potentials (Fig. 2 *C*). Both the speed of activation and the maximum number of channels open increase with depolarization. The averaged currents resemble in their time course the macroscopic K currents recorded from perfused squid giant axons under similar ionic conditions (cf. Bezanilla and Armstrong, 1972).

Single-Channel Patches: Small-Conductance Channel

In order to increase the probability of obtaining patches in which only one active channel was present, we often resorted to recording under conditions in which most

of the channels were in an inactivated state. Fig. 3 *A* shows single-channel records from a patch maintained at a relatively depolarized holding potential of −30 mV. Channels were activated by depolarizing pulses to 50 mV, which were preceded by 50-ms pulses to −80 mV to remove some steady state inactivation. With this type of stimulating protocol, single-channel currents were more readily resolved. The channels open with a very short latency after the beginning of the pulse and fluctuate rapidly between the open and closed levels through the duration of the pulse. The averaged current obtained from 48 records at this potential (Fig. 3 *A*, upper trace) reaches its steady state level within 5 ms and is maintained during the duration of the pulse, as expected from the activation of the "delayed rectifier" K channels in this preparation. The amplitude histogram of all data points (Fig. 3 *B*) was fitted well

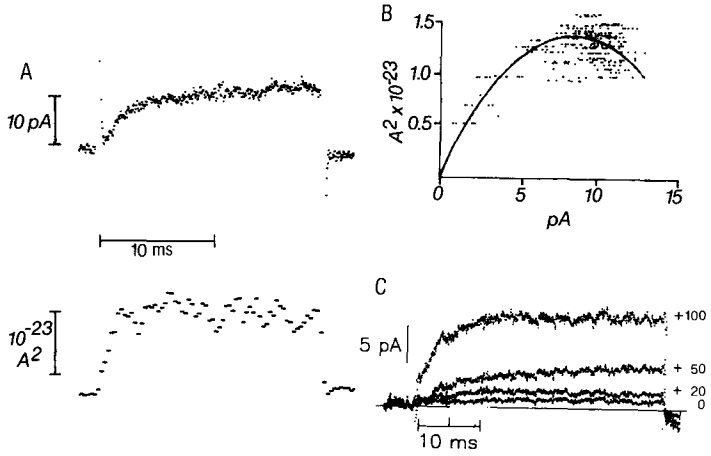

FIGURE 2. Multichannel patches. (*A*) Mean current (upper trace) and associated ensemble variance (lower trace) calculated from 200 depolarizations to 80 mV. The holding potential was −80 mV and the solutions were 10 K ASW//400 K. (*B*) Plot of variance as a function of mean current, from the experimental data presented in *A*. The dots correspond to data points; the solid line corresponds to the fit to the function $S^2 = (iI) - (I^2/N)$, with $i = 2.7$ and $N = 8$. (*C*) Currents obtained from the average of 32–65 pulses to the potentials indicated in front of each trace. The holding potential was −70 mV. This is a different patch from that shown in *A* and *B*. The solutions were 5 K ASW//285 K and the temperature was 19°C.

by the sum of two Gaussian distributions. The value of single-channel current estimated from the fit was 2.7 pA, corresponding to a single-channel conductance of 20 pS. This value is in good agreement with that derived from the ensemble fluctuation analysis described above. Determination of the number of active channels is rendered difficult by the presence of slow inactivation. In this particular patch, no double openings were seen at 50 mV, although they were observed when the membrane potential was stepped to 100 mV. If one considers that the pattern of activity observed at 50 mV is due to one active channel (the other being in a slow-inactivated state), the probability of being open calculated from the relative areas of the amplitude histogram would be 0.9.

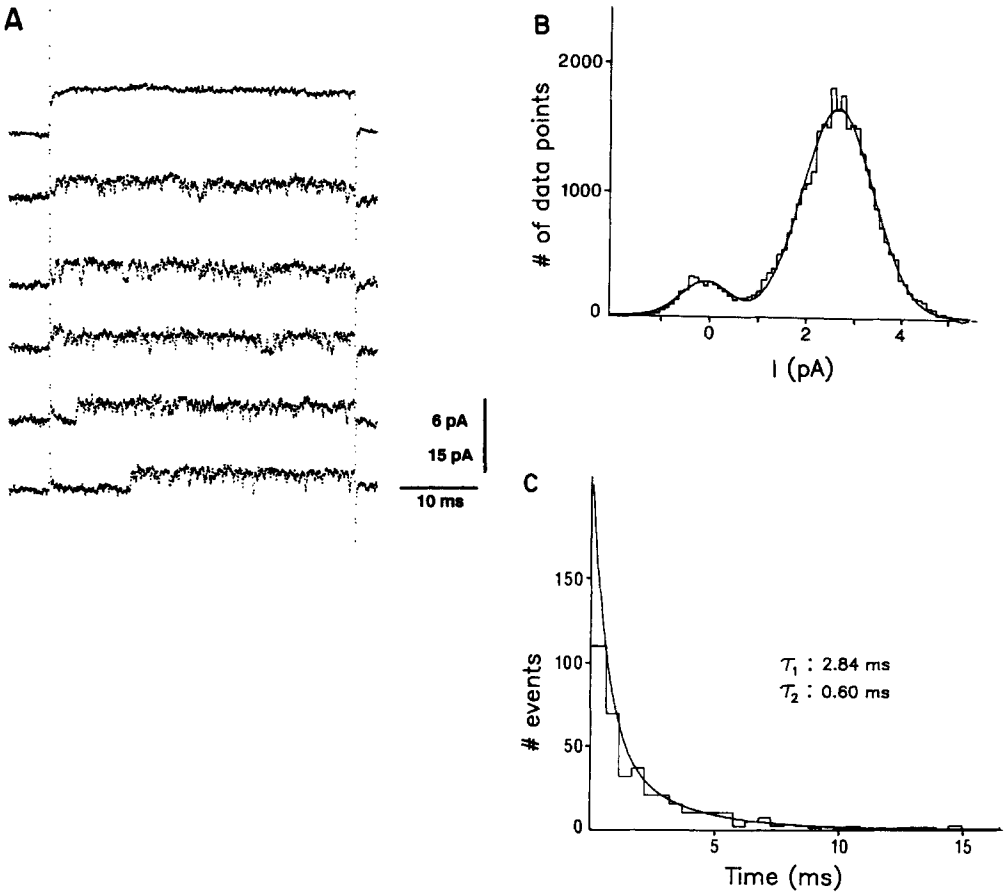

FIGURE 3. Properties of the small-conductance channel. (*A*) Single-channel currents recorded during pulses to 50 mV. The holding potential was −30 mV; depolarizing pulses were preceded by 50-ms pulses to −80 mV. The upper trace presents the average current from 48 out of a total of 93 pulses. The solutions were 5 K ASW//528 K and the temperature was 13°C. The 15-pA calibration corresponds to the single-channel traces and the 6-pA calibration corresponds to the averaged current. (*B*) Amplitude histogram of all data points from the set of pulses to 50 mV. The solid line corresponds to the fit of experimental data with the sum of two Gaussian distributions. Fit parameters (x_k, b_k, a_k): −0.12 pA, 0.708 pA, 268.3; 2.60 pA, 1.02 pA, 1,635. (*C*) Histogram of open times from the same set of data. The solid line corresponds to the fit with two exponentials. Fit parameters (time constant, number of events): 0.6 ms, 154; 2.84 ms, 48.2.

Fig. 3 *C* presents a histogram of open times for the channels activated by pulses to 50 mV. Two exponentials, with time constants of 2.84 and 0.6 ms, were required to fit this histogram. The double-exponential nature of the histogram, however, may result from the contribution of more than one channel to the records. Even though no double levels were observed at this potential, this possibility cannot be eliminated. An estimate of the mean open time, obtained by adding the total time the

channel is open and dividing by the number of open-to-closed transitions, yielded a value of 2.1 ms.

Single-Channel Patches: Large-Conductance Channel

Under similar ionic and recording conditions, many experiments revealed another distinct type of single-channel activity. This channel differs from the 20-pS channel

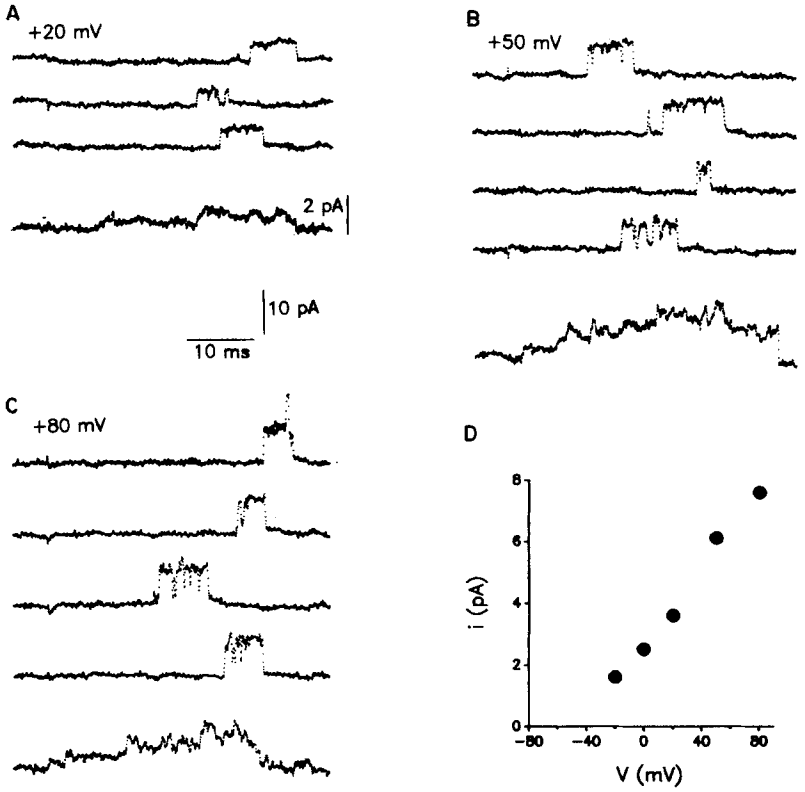

FIGURE 4. Large-conductance channel. (*A–C*) Single-channel currents and the corresponding average (lower traces in each panel) resulting from pulses to the indicated potentials. The holding potential was −30 mV; depolarizing pulses were preceded by 50-ms pulses to −80 mV. Averaged currents include only pulses that showed channel activity. The 10-pA calibration bar applies to the single-channel traces; the 2-pA bar corresponds to the averaged traces. The solutions were 5 K ASW//528 K; the temperature was 13°C. (*D*) Current-voltage relation for the experiment illustrated in *A–C*. Single-channel currents were derived from Gaussian fits to amplitude histograms.

described above in the value of its single-channel conductance, its kinetic properties, and its probability of being open. The activity of this channel varied from patch to patch: in some instances, the channel was extremely active and in others it showed a very low probability of being open. An example of one type of activity shown by this channel in response to pulses to three different membrane potentials is presented in Fig. 4, *A–C*. The upper traces in each panel correspond to selected sweeps; the

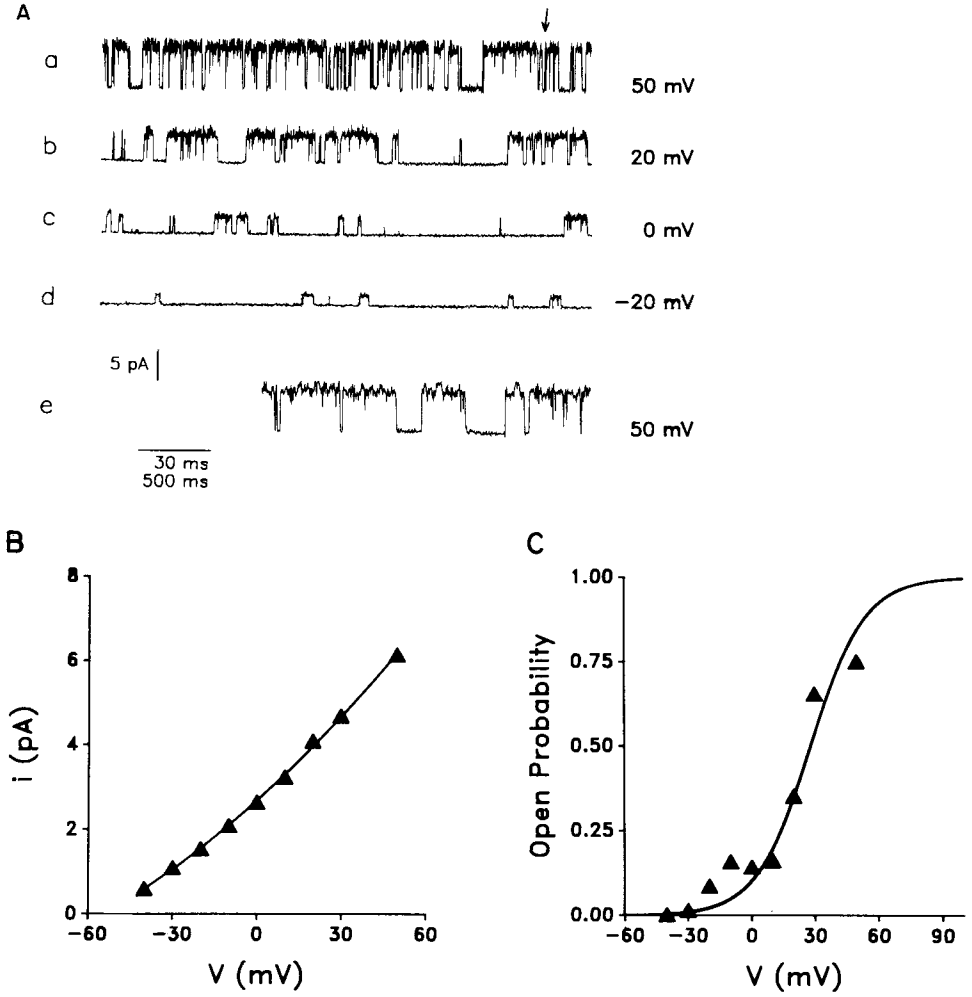

FIGURE 5. Steady state properties of the large-conductance channel. (*A*) Single-channel recordings at the indicated holding potentials. The solutions were 10 K ASW//525 K. The temperature was 21.5°C. Trace *e* is taken from trace *a* (indicated by the arrow in *a*) and plotted on an expanded time scale to illustrate the higher conductance level. The 30-ms scale bar corresponds to trace *e*; the 500-ms scale bar corresponds to traces *a–d*. (*B*) Current-voltage relation for the single-channel events illustrated in *A*. (*C*) Probability of being open vs. voltage. Open probabilities were determined from the equation $A/(A + B)$, where A is the total time spent in the open state and B is the total time spent in the closed state. For each holding potential, 1 s worth of recordings was analyzed. Same patch as shown in panels *A* and *B*.

lower traces correspond to the averaged currents obtained from the ensemble of all sweeps in which openings of this channel type were detected. In the experiment shown in Fig. 4, openings caused by this channel occurred late after pulse onset and with a very low probability, even at high membrane depolarizations (in this patch, only 11 traces out of 34 showed openings of this channel type at 50 mV). Furthermore, reconstructions of the large-conductance channel with this type of activity showed a pronounced lag in the activation time course. Fig. 4 *D* presents the current-voltage relation for the channel illustrated in *A–C*. The conductance ranges from 25 pS at −20 mV to 46 pS at 80 mV.

This large-conductance channel showed a strikingly different type of gating behavior in other patches recorded under similar ionic conditions. For example, Fig. 5 illustrates the activity of another one of these channels, which had a relatively high probability of being open. The steady state activity of this channel at four different membrane potentials is shown in Fig. 5 *A*(*a–d*). The current-voltage relation from this experiment is shown in Fig. 5 *B*. The conductance is 14 pS at −40 mV and 46 pS at 50 mV, in excellent agreement with the current-voltage relation for the channel activity shown in Fig. 4. The channel frequently went into a higher-conductance state at more positive potentials. This was most clearly seen at a holding potential of 50 mV where transitions were observed between a conductance of 46 pS and a higher value of 60 pS (see Fig. 5 *A*, *e*). Transitions to this higher-conductance level were seen only when the channel was open; that is, no comparable transitions were observed from the baseline.

In contrast to the 20-pS channel, this large-conductance channel could be elicited upon sustained depolarization and remained active for several minutes at all holding potentials. However, at more positive potentials, the channel occasionally went into silent periods. For example, at a holding potential of 50 mV during a recording period of 26 s, channel activity stopped completely for 7.4 s. As described in the Methods, such periods were not included in the determination of open probability. The steady state probability of being open for the large-conductance (40 pS) channel in the high activity state illustrated in Fig. 5 *A* is plotted as a function of membrane potential in Fig. 5 *C*. The steady state probability of this channel being open, which reached a value of 0.75 at 50 mV, is much higher than that observed in other experiments (see, for example, Figs. 4 and 7). The probability of being open for the channel activity shown in Fig. 4 was 0.16 excluding blank traces, and 0.06 including blank traces for 40-ms pulses to 50 mV.

The kinetics of opening and closing of the large-conductance channel in the high activity state shown in Fig. 5 were characterized in more detail (Fig. 6). The distribution of open times could be described by the sum of two exponentials (Fig. 6 *A*, left panel). Two exponentials often provided a reasonable description of the closed-time histograms, although, at high membrane potentials (30 and 50 mV), a third, faster exponential was needed to yield a good fit (Fig. 6 *B*, right panel). The resultant open-time constants were plotted against steady state membrane potential (Fig. 6 *B*, left panel). Both the slow and fast time constants increased with membrane potential up to 0 and 20 mV, respectively. At higher membrane potentials, the open-time constant decreased with increasing potential, particularly the slower time constant. This would be expected from the increased flickering of the channel seen at the

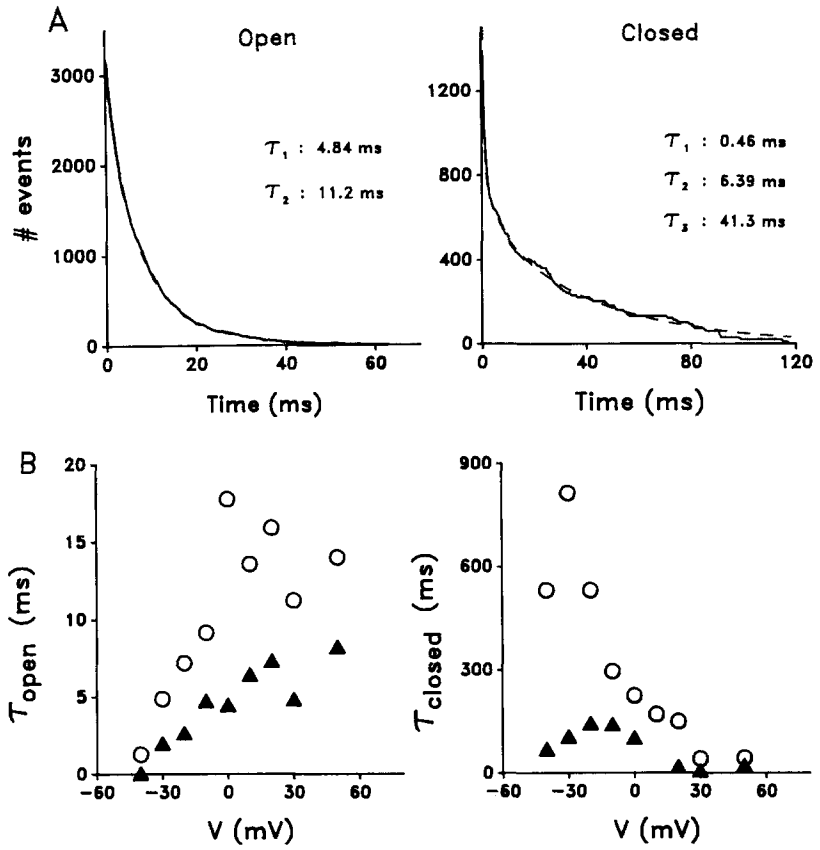

FIGURE 6. Steady state kinetic properties of the large-conductance channel. (*A*) Histograms of open (left panel) and closed (right panel) times. The solid line corresponds to the data and the dashed line corresponds to the fit of the data with two (left) and three (right) exponentials. The holding potential was 30 mV, the temperature was 21.5°C, and the solutions were 10 K ASW//525 K. Fit parameters for the open-time histogram (time constant, number of events): 4.84 ms, 1,652; 11.2 ms, 1,408. Fit parameters for the closed-time histogram (time constant, number of events); 0.46 ms, 1,585; 6.39 ms, 279; 41.2 ms, 571. (*B*) Open-time constants (left) and closed-time constants (right) are shown as a function of membrane potential. Plotted are the time constants obtained from fits like those illustrated in panel *A*. The fast open-time constant at −20 mV was 0.07 ms; the fast closed-time constant at 30 mV was 6.4 ms. Same patch as illustrated in panel *A* and in Fig. 5.

higher potentials. The increase in the fast open-time constant at 50 mV could be due to brief, undetected closings. At more positive membrane potentials, the transitions between open and closed states are very fast, and brief closing events may not have been resolved with the 5-kHz recording bandwidth used; the resultant time constants are thus likely to be slower than expected. In Fig. 6 *B* (right panel), the time constants for closing are plotted against steady state membrane potential. The slower closed-time constant was much more voltage dependent than the faster time

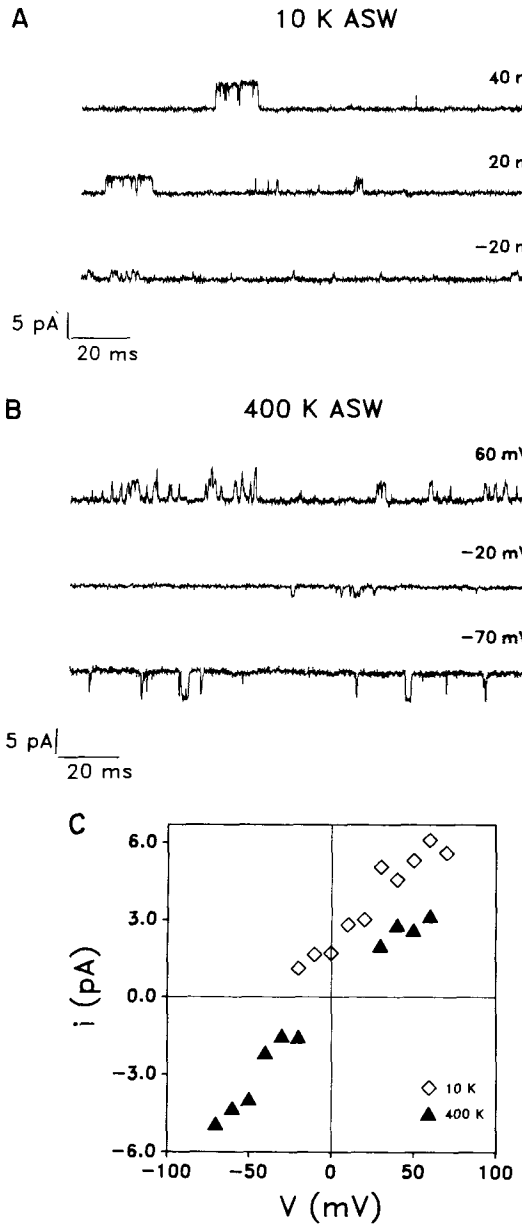

FIGURE 7. Selectivity of the large-conductance channel. (*A*) Single-channel events, recorded in normal 10 K ASW, at the indicated holding potentials. The solutions were 10 K ASW//525 K and the temperature was 25°C. (*B*) Same patch as illustrated in panel *A*, after the external solution had been changed to 400 K ASW. The internal solution remained 525 K and the temperature was 25°C. (*C*) Current-voltage relation for the experiment illustrated in panels *A* and *B*. Open diamonds: 10 K ASW; filled triangles: 400 K ASW.

constant for closing. The slow time constant decreased markedly with increasing membrane potential as the time the channel spent in the open state increased. The fast time constant increased slightly with increasing potential up to −10 mV and then decreased with further increases in membrane potential. Both the slow and the fast time constants for closing increased slightly at 50 mV; again, this might be due to brief, undetected closings, as discussed above.

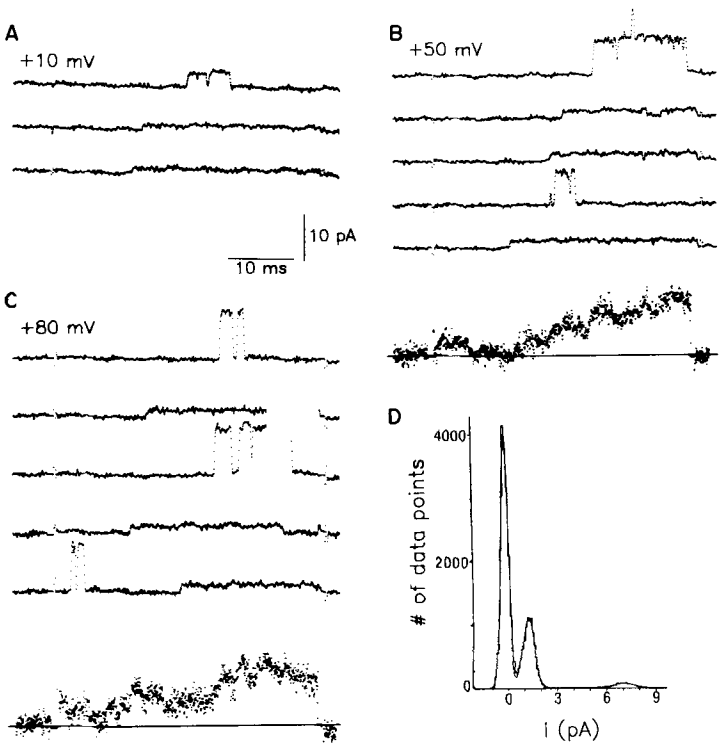

FIGURE 8. Large-conductance channel following removal of K^+. (*A–C*) Single-channel events and averaged currents (lower traces in *B* and *C*) activated by pulses to the indicated potentials. The patch was obtained from an axonal sheet that had been exposed to 0 K ASW for 20 min. The holding potential was −70 mV, the solutions were 0 K ASW//528 K, and the temperature was 17°C. (*D*) Amplitude histogram of all data points from the same patch at 50 mV. The solid line corresponds to the fit of three Gaussian distributions. Fit parameters (x_k, b_k, a_k): −0.15 pA, 0.315 pA, 4,022; 1.26 pA, 0.495 pA, 1,090; 6.97 pA, 0.85 pA, 70.

The large-conductance channel is very sensitive to the external concentration of K ions and thus appears to be highly selective for K ions (Fig. 7). Examples of channel activity recorded in 10 mM external K (10 K ASW) are shown for three membrane potentials in Fig. 7 *A*. In Fig. 7 *B*, examples of the activity on this same channel are shown after the external solution was changed to one containing 400 mM K (400 K ASW). The single-channel events recorded in 10 K ASW were outward for all membrane potentials shown, from −20 to 60 mV. However, in 400 K ASW, the single-channel events were inward from −70 to −20 mV and outward at 60 mV. These

results can be seen more clearly in Fig. 7 *C*, where single-channel current is plotted against steady state membrane potential in 10 K and 400 K ASW. The chord conductance in 10 K ASW was 18 pS at −20 mV and 43 pS at 60 mV. In 400 K ASW, the chord conductance was 78 pS at −70 mV and 54 pS at 30 mV. The slope conductance was 58 pS in 10 K ASW and 64 pS in 400 K ASW. The reversal potential determined by extrapolation of the current-voltage relation was approximately −50 mV in 10 K ASW and 3.2 mV in 400 K ASW. This shift in the zero current potential toward more positive potentials would be expected if the channel is selective for K over Na.

Removal of External K^+ Alters K Channel Activity

In the perfused squid axon, removal of K^+ from both sides of the membrane leads to a gradual decline in the size of the K currents measured after reintroduction of

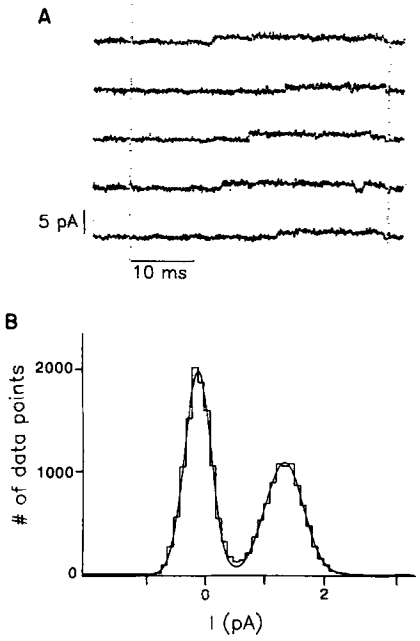

FIGURE 9. Effects of K^+ removal on the single-channel current. (*A*) Single-channel currents recorded for pulses to 50 mV in a patch obtained from an axonal sheet that had been maintained in 0 K ASW for 20 min. The holding potential was −70 mV, the solutions were 0 K ASW//528 K, and the temperature was 17°C. (*B*) Amplitude histogram of all data points from the pulses to 50 mV. Solid line corresponds to the fit of two Gaussian distributions. Fit parameters (x_k, b_k, a_k): −0.15 pA, 0.31 pA, 1,953; 1.29 pA, 0.45 pA, 1,077.

a normal K^+ concentration (Chandler and Meves, 1970; Almers and Armstrong, 1980). We thought that exposure of the axonal sheets to ASW without K^+ (0 K ASW) for short periods of time might aid in decreasing the number of functional channels. The axon was cut open and bathed in 10 K ASW for times ranging between 8 and 20 min. While 0 K ASW was maintained in the bath, a patch pipette was approached to the membrane and a seal was formed.

The properties of the 40-pS channel did not appear to be affected by exposure of the axonal sheet to 0 K ASW. This is illustrated by the records shown in Fig. 8, obtained from a patch exposed to 0 K ASW for 20 min. This patch displayed normal activity of the large-conductance channel, in addition to a small-conductance channel, which will be described below. Under these conditions, averaged currents

(lower traces in each panel) show an activation time course with a long lag after pulse onset, reiminiscent of the reconstruction sometimes obtained from the activity of the large-conductance channel under normal conditions (e.g., Fig. 4).

The 20-pS channel, on the other hand, was rarely observed after exposure of the axonal sheet to 0 K ASW. This is in striking contrast to the results in 5–10 K ASW, where the 20-pS channel is seen more frequently than the 40-pS channel.

A third type of unitary channel activity was frequently observed following exposure to 0 K ASW. As illustrated by the records presented in Fig. 9 *A*, this channel has a longer latency before opening and shows less flickering activity than that recorded from axonal sheets maintained in K-containing ASW (Figs. 3 and 4). Furthermore, the single-channel conductance is significantly lower than the other two channels, ranging between 8 and 10 pS. The overall probability of being open, estimated by the relative amplitude of the peaks of the amplitude histogram (see Fig. 9 *B*), was found to be lower than that of the 20-pS channel. At 50 mV, this value was 0.3, in contrast to a value of 0.9 for the 20-pS channel recorded from patches in 5 K ASW.

DISCUSSION

The results presented in this article demonstrate the existence of at least two distinct types of K channels in the squid giant axon. These channels differ in their single-channel conductance as well as in their gating properties. In addition, a third type of channel activity was found in axons exposed to 0 K ASW. The value of single-channel conductance of 19–20 pS that we report for the low-conductance channel is somewhat larger than that predicted from the study of Conti and Neher (1980) in perfused squid axons maintained in an inverted K^+ gradient. Under those conditions, these authors measured a single-channel conductance of 17.5 pS, and extrapolated to a value of 9–11 pS in physiological solutions. A possible explanation for the difference in single-channel conductance is that in their study the internal solution contained Na, which blocks K conductance (Bezanilla and Armstrong, 1972). On the other hand, their value is comparable to the 8–10-pS channel we observed after exposure to 0 K ASW.

On the basis of our results, it is possible that the 20-pS channel may be the main contributor to the delayed rectifier conductance normally studied in the squid axon. The agreement of the fit of the relation between ensemble variance and mean current to a model which assumes that channels are identical and independent suggests that, under normal ionic conditions (high K^+ inside and low K^+ outside), macroscopic currents elicited by relatively short depolarizations are largely comprised of the 20-pS channel. This is supported by comparisons of the time course of the current obtained by averages of depolarization-activated, 20-pS single-channel events with the averaged traces obtained in multichannel patches. In both cases, the resulting current shows an activation time course reminiscent of the delayed rectifier K currents in this preparation. Furthermore, as expected from the macroscopic current (Ehrenstein and Gilbert, 1966; Chabala, 1984), the single-channel events show no inactivation during pulses of 20–100 ms duration, but can be rendered refractory to activation by holding the membrane potential at depolarized levels for sev-

eral seconds. Other estimates of the single-channel conductance of delayed rectifier channels in excitable cells are similar to that reported here for the 20-pS channel. For example, a value of 15 pS has been obtained for the skeletal muscle delayed rectifier channel (Standen et al., 1985).

It is possible, however, that the 40-pS channel also contributes to the total macroscopic current obtained with short depolarizations. Although its single-channel conductance is significantly larger than that of the 20-pS channel, this channel often opens infrequently during depolarizing pulses. Occasionally, however, its opening probability is higher. In these cases, it would make a larger contribution to macroscopic K currents. It is likely, then, that the delayed rectifier conductance is a composite of at least two K channel types. Further work is needed to define the contribution of the various channel activities to the macroscopic current.

A sequential kinetic scheme involving several closed states and a single open state has been used to model the process of activation of the delayed rectifier K conductance in squid axon. On the basis of studies of the macroscopic currents (Gilly and Armstrong, 1982) as well as of gating currents (White and Bezanilla, 1985), it has been proposed that the transition between the last closed state and the open state is not rate-limiting in this process. In accord with the observations of Conti and Neher (1980), the present results for both the 20-pS and the 40-pS channel show that, once open, these channels flicker rapidly between the closed and open levels. This type of behavior is consistent with the hypothesis of a fast transition between the last closed state and the open state of the channel.

Our attempts to reduce the density of K channels by depriving the axonal sheets of K^+ for short periods of time yielded somewhat surprising results. Previous studies (Chandler and Meves, 1970; Almers and Armstrong, 1980) have shown that this procedure leads to a gradual and irreversible loss of K currents, the remaining K current displaying unaltered kinetics. Our observations suggest that the 20-pS channels are functionally lost when both sides of the membrane are exposed to K-free solutions, while a channel with a smaller conductance (10 pS) and "modified" kinetic properties is revealed by this treatment. In all patches studied, the probability of finding this 10-pS channel open in 0 K ASW was lower than that observed for the 20-pS channel in K-containing ASW. It is thus likely that macroscopic current measurements would fail to detect currents caused by the activity of this channel.

Our results do not allow us to determine whether the small, 10-pS conductance channel is the result of a modification of one of the K channels or a new type of channel altogether. Because we were unable to detect activity of the 20-pS channel after K deprivation, it is possible that the 10-pS channel is a modified form of the 20-pS channel. It has been proposed (Almers and Armstrong, 1980) that, in the absence of permanent cations, the K channels are destabilized by the electrostatic forces generated by negative charges within the channel that are normally counteracted by resident cations. It is possible that this process of destabilization could lead to a gradual loss of some of the voltage-dependent gating sensitivity (thus leading to a longer lag time and lower probability of opening) as well as a decrease in the open-channel conductance. The fact that the large-conductance channel is unaltered by K deprivation indicates that this channel clearly does not require the presence of permeant cations to survive. Alternatively, it is possible that the 10-pS chan-

nel is present under normal conditions, but exposure of the axonal sheet to 0 K ASW increases the probability of seeing this channel. Consistent with this explanation, the 10-pS channel has occasionally been observed when the axonal sheet is exposed to 10 K ASW.

In conclusion, the results presented in this article show that patch-recording techniques can be successfully applied to the cut-open axon preparation. The implementation of this technique should yield useful data to complement the wealth of information that has been derived from measurements of macroscopic ionic currents and of gating currents in this preparation. Recording of ionic currents from excised patches containing one or a few K channels also offers the advantage of eliminating certain errors, such as the accumulation of K^+ in the periaxonal space (Frankenhaeuser and Hodgkin, 1956; Adelman et al., 1973), that make interpretation of macroscopic K currents challenging.

Many thanks to Drs. G. Augustine and C. Vandenberg for reading and commenting on this manuscript.

This work was supported by U.S. Public Health Service grant GM-30376 and by the Muscular Dystrophy Association of America.

Original version received 9 October 1987 and accepted version received 28 December 1987.

REFERENCES

Adelman, W. J., Jr., Y. Palti, and J. P. Senft. 1973. Potassium ion accumulation in a periaxonal space and its effect on the measurement of membrane potassium ion conductance. *Journal of Membrane Biology.* 13:387–410.

Almers, W., and C. M. Armstrong. 1980. Survival of K^+ permeability and gating currents in squid axons perfused with K^+-free media. *Journal of General Physiology.* 75:61–78.

Armstrong, C. M. 1981. Sodium channels and gating currents. *Physiological Reviews.* 61:644–683.

Bezanilla, F. 1985*a*. Gating of sodium and potassium channels. *Journal of Membrane Biology.* 88:97–111.

Bezanilla, F. 1985*b*. A high capacity data recording device based on a digital audio processor and a video cassette recorder. *Biophysical Journal.* 47:437–441.

Bezanilla, F. 1987. Single sodium channels from the squid giant axon. *Biophysical Journal.* 52:1087–1090.

Bezanilla, F., and C. M. Armstrong. 1972. Negative conductance caused by the entry of sodium and cesium ions into the potassium channels of the squid axons. *Journal of General Physiology.* 60:588–608.

Chabala, L. D. 1984. The kinetics of recovery and development of potassium channel inactivation in perfused squid (*Loligo pealei*) giant axon. *Journal of Physiology.* 356:193–220.

Chandler, W. K., and H. Meves. 1970. Sodium and potassium currents in squid axons perfused with fluoride solutions. *Journal of Physiology.* 211:623–652.

Conti, F., and E. Neher. 1980. Single channel recording of K^+ currents in squid axons. *Nature.* 285:140–143.

Ehrenstein, G., and D. L. Gilbert. 1966. Slow changes of potassium permeability in the squid giant axon. *Biophysical Journal.* 6:553–566.

Frankenhauser, B., and A. L. Hodgkin. 1956. The after-effects of impulses in the giant nerve fibers of *Loligo*. *Journal of Physiology.* 131:341–376.

Gilly, W. F., and C. M. Armstrong. 1982. Divalent cations and the activation kinetics of potassium channels in squid giant axons. *Journal of General Physiology.* 79:965–996.

Hamill, O. P., A. Marty, E. Neher, B. Sakmann, and F. J. Sigworth. 1981. Improved patch-clamp techniques for the recording from cell and cell-free membrane patches. *Pflügers Archiv.* 391:85–100.

Hodgkin, A. L., and A. F. Huxley. 1952. A quantitative description of membrane current and its application to conduction and excitation in nerve. *Journal of Physiology.* 117:500–544.

Hodgkin, A. L., and B. Katz. 1949. The effect of calcium on the axoplasm of giant nerve fibres. *Journal of Experimental Biology.* 26:292–294.

Latorre, R., and C. Miller. 1983. Conduction and selectivity in potassium channels. *Journal of Membrane Biology.* 71:11–30.

Levis, R. A., F. Bezanilla, and R. M. Torres. 1984. Estimate of the squid axon sodium channel conductance with improved frequency response. *Biophysical Journal.* 45:11*a*. (Abstr.)

Llano, I., and F. Bezanilla. 1980. Current recorded from a cut-open giant axon under voltage clamp. *Proceedings of the National Academy of Sciences.* 77:7484–7486.

Llano, I., and F. Bezanilla. 1985. Two types of potassium channels in the cut-open squid giant axon. *Biophysical Journal.* 47:221*a*. (Abstr.)

Pant, H. C., and H. Gainer. 1980. Properties of a calcium-activated protease in squid axoplasm which selectively degrades neurofilament proteins. *Journal of Neurobiology.* 11:1–12.

Sigworth, F. J. 1980. The variance of sodium current fluctuations at the node of Ranvier. *Journal of Physiology.* 307:97–129.

Sigworth, F. J. 1983. Electronic design of the patch clamp. *In* Single-Channel Recording. B. Sakmann and E. Neher, editors. Plenum Publishing Corp., New York, NY. 3–35.

Stimers, J. R., F. Bezanilla, and R. E. Taylor. 1987. Sodium channel gating current. Origin of the rising phase. *Journal of General Physiology.* 89:521–540.

Standen, N. B., P. R. Stanfield, and T. A. Ward. 1985. Properties of single potassium channels in vesicles formed from the sarcolemma of frog skeletal muscle. *Journal of Physiology.* 364:339–358.

White, M. M., and F. Bezanilla. 1985. Activation of squid axon K^+ channels. Ionic and gating current studies. *Journal of General Physiology.* 85:539–554.